

Spatial Language Understanding for Object Search in Partially Observed Cityscale Environments

Kaiyu Zheng, Deniz Bayazit, Rebecca Mathew, Ellie Pavlick, Stefanie Tellex¹

Abstract—We present a system that enables robots to interpret spatial language as a distribution over object locations for effective search in partially observable cityscale environments. We introduce the spatial language observation space and formulate a stochastic observation model under the framework of Partially Observable Markov Decision Process (POMDP) which incorporates information extracted from the spatial language into the robot’s belief. To interpret ambiguous, context-dependent prepositions (e.g. *front*), we propose a convolutional neural network model that learns to predict the language provider’s relative frame of reference (FoR) given environment context. We demonstrate the generalizability of our FoR prediction model and object search system through cross-validation over areas of five cities, each with a 40,000m² footprint. End-to-end experiments in simulation show that our system achieves faster search and higher success rate compared to a keyword-based baseline without spatial preposition understanding.

I. INTRODUCTION

Consider the scenario in which a tourist is looking for an ice cream truck in an amusement park. She asks a passer-by and gets the reply *the ice cream truck is behind the ticket booth*. The tourist looks at the amusement park map and locates the ticket booth. Then, she is able to infer a region corresponding to that statement and find the ice cream truck, even though the spatial preposition *behind* is inherently ambiguous and subjective to the passer-by. Such spatial language understanding is important in robot applications such as search and rescue when an untrained operator communicates with the robot via natural language.

This problem is challenging because humans produce diverse spatial language phrases based on their observation of the environment and knowledge of target locations, yet none of these factors are available to the robot. In addition, the robot may operate in a different area than where it was trained. The robot must generalize its ability to understand spatial language across environments.

Existing approaches to spatial language understanding from formal semantics [1, 2] often assume referenced objects already exist in the agent’s world model. Unfortunately, real world environments are often partially observable and the robot does not have a complete world model. Other works that do consider partial observability [3, 4, 5] deal with languages that do not involve ambiguous spatial prepositions or assume a robot-centric frame of reference. This leads to systems that have limited ability to understand diverse spatial relations that provide critical disambiguating information, such as *behind the ticket booth*.

¹ Brown University, Providence, RI, 02912, USA. Emails: {kaiyu.zheng, deniz_bayazit, rebecca_mathew, ellie_pavlick}@brown.edu, stefie10@cs.brown.edu

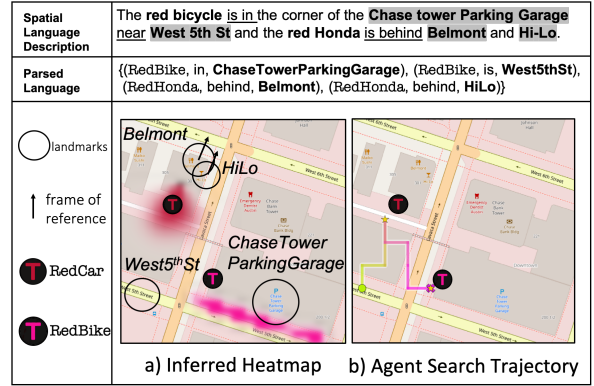


Fig. 1: Our system first automatically parses a given spatial language into a set of atomic propositions then predicts the frame of references (FoR) for predicates such as *behind*. These propositions and FoRs are interpreted through a stochastic observation model and integrated into the robot’s belief state. The resulting belief over target locations is shown in (a), and the object search trajectory (from green to pink) is shown in (b).

To deal with partial observability of the referenced object, we introduce a novel spatial language observation space and formulate a stochastic spatial language observation model in the Partially Observable Markov Decision Process (POMDP) framework [6] that enables the robot to incorporate into its belief state, via belief update, the spatial information about the referenced object extracted from natural language. To understand ambiguous, context-dependent prepositions such as *behind*, we develop a novel convolutional neural network that infers the latent frame of reference (FoR) given an egocentric synthetic image of the referenced landmark and surrounding context. The predicted FoR is integrated into the spatial language observation model. After the initial belief update, the robot proceeds to search according to a policy produced by a POMDP solver. Our system enables robots to interpret spatial language and perform search more effectively in cityscale environments.

We evaluate both the FoR prediction model and end-to-end performance with language data collected from areas of five cities. Five-fold cross-validation is employed to test the generalizability of our method. We show that our system finds objects faster and attains higher success rate by exploiting spatial information from language compared to a baseline that does not interpret spatial language. This baseline uses the same parsing pipeline but a keyword-based model proposed in [5], which assigns uniform probability over referenced landmarks. Finally, we report results for varying language complexity and spatial prepositions to discuss advantages and limitations of our approach.

II. RELATED WORK

Language grounding aims to map symbols of language to concepts and structures in the world available to the agent. Most work on spatial language grounding assumes a fully observable domain where the references are known or within the field of view of the robot [1, 2, 7, 8]. Spatial language understanding in partially observable environments is an emerging area of study [3, 4, 5, 9]. Thomason et al. [9] propose a domain where the robot has access to a dialogue between humans discussing the location of the target prior to searching. Hemachandra et al. [3] and Patki et al. [4] learn to infer a distribution over semantic maps from given language for instruction following and plan actions through behavior inference. These instructions are typically FoR-independent or involve only the robot’s own FoR. In contrast, we study language descriptions with FoRs relative to referenced landmarks and produce policy via online planning. Wandzel et al. [5] propose the Object-Oriented POMDP framework for object search and a proof-of-concept keyword-based model for language understanding in indoor space. Our work handles diverse spatial language using a novel spatial language observation model and focuses on search in cityscale environments. We evaluate our system against a keyword-based baseline similar to the one in [5].

Cognitive scientists have grouped FoRs into three categories: absolute, intrinsic, and relative [10, 11]. Absolute FoRs (e.g. for *north*) are fixed and depend on the agreement between speakers of the same language. Intrinsic FoRs (e.g. for *at the door of the house*) depend only on properties of the referenced object. Relative FoRs (e.g. for *behind the ticket booth*) depend on both properties of the referenced object and the perspective of the observer. In this paper, spatial descriptions are provided by human observers who may impose relative FoRs or absolute FoRs.

III. PROBLEM SETTING

A robot is tasked to search for a number of target objects in an urban area represented as a discretized 2D map of landmarks. The robot is equipped with the map and an on-board sensor capable of detecting the targets within the field of view. However, the robot has no knowledge of object locations a priori, and the map size is substantially larger than the sensor’s field of view, making brute-force search infeasible. A human with access to the same map and prior knowledge of object locations provides the robot with a natural language description. For example, given the map in Figure 1, one could say *the red Honda is behind Belmont, near Hi-Lo*. The language is assumed to mention some of the target objects and their spatial relationships to some of the known landmarks, yet there is no assumption about how such information is described. To be successful, the robot must incorporate information from spatial language to efficiently search the environment until it finds the target object.

IV. APPROACH

Spatial language is useful for efficient object search but could also be ambiguous or misleading. Therefore, we regard

it as a stochastic observation in the POMDP framework incorporated into the robot’s belief. In this section, we first briefly review POMDP and the multi-object search (MOS) task proposed in [5]. Then, we present our approach consisting of three parts: spatial language observation modeling, FoR prediction and spatial information extraction.

A. POMDP and Multi-Object Search

POMDP [6] is a framework to describe sequential-decision making problems where the agent does not fully observe the environment state. Formally, a POMDP is defined as a tuple $\langle \mathcal{S}, \mathcal{A}, \Omega, T, O, R, \gamma_d \rangle$. Given an action $a \in \mathcal{A}$, the environment state transitions from $s \in \mathcal{S}$ to $s' \in \mathcal{S}$ following the transition function $T(s, a, s') = \Pr(s'|s, a)$. The agent receives an observation $o \in \Omega$ according to the observation model $O(s', a, o) = \Pr(o|s', a)$, and an expected reward $r = R(s, a, s')$. The agent maintains a *belief state* $b_t(s) = \Pr(s|h_t)$ which is a sufficient statistic for the history $h_t = (ao)_{1:t-1}$. The agent updates its belief given the action and observation by $b_{t+1}(s') = \eta O(s', a, o) \sum_s T(s, a, s') b_t(s)$ with a normalizing constant η . The objective is to find a policy $\pi(b_t)$ which maximizes the expected discounted future rewards with a discount factor γ_d .

In MOS [5], the task is to search for N targets in a discrete 2D map \mathcal{M} that contains landmark information. The state is defined as $s = (s_1, \dots, s_N, s_r, \mathcal{M})$, where $s_i = (x_i, y_i)$ is the state for target i , $1 \leq i \leq N$. Robot state $s_r = (x, y, \theta, \mathcal{F})$ consists of its pose (x, y, θ) and a set of found targets $\mathcal{F} \subseteq \{1, \dots, N\}$. The optimal policy moves the robot to explore areas in the map that it thinks are likely to contain the object, based on a belief state that boils down to a distribution over target locations in the map. The belief state is updated using observations from its sensors and also from spatial language. We focus on formalizing the spatial language observation in the following section.

B. Integrating Spatial Language into POMDPs

According to Landau and Jackendoff [12], the standard linguistic representation of an object’s place requires three elements: the object to be located (*figure*), the reference object (*ground*), and their relationship (*spatial relation*), which in our case is a spatial preposition. We abide by this convention and represent spatial information from a given natural language description in terms of atomic propositions, each represented as a tuple of the form (f, r, γ) , where f is the *figure*, r is the *spatial relation* and γ is the *ground*. In our case, f refers to a target object, γ refers to a landmark on the map, and r is a predicate that is true if the locations of f and γ satisfy the semantics of the spatial relation. As an example, given spatial language *the red Honda is behind Belmont, near Hi-Lo*, two tuples of this form can be extracted: $\{(\text{RedCar}(f), \text{behind}(r), \text{Belmont}(\gamma)), (\text{RedCar}(f), \text{near}(r), \text{HiLo}(\gamma))\}$.

We define the *spatial language observation* as a set of (f, r, γ) tuples extracted from a given spatial language. The space of all possible tuples of such form for a given map is the *spatial language observation space*. Next, we formulate the corresponding observation model.

We denote a spatial language observation as $o_{\mathcal{R}}$. We can split $o_{\mathcal{R}}$ into subsets, $o_{\mathcal{R}} = \cup_{i=1}^N o_{\mathcal{R}_i}$, each $o_{\mathcal{R}_i} = \cup_{j=1}^{|o_{\mathcal{R}_i}|} (f_i, r_j, \gamma_j)$ is the set of tuples where the figure is target object i . Since the human describes the target objects with respect to landmarks on the map, the spatial language is conditionally independent from the robot state and action given the map \mathcal{M} and the target locations s'_1, \dots, s'_N . Therefore, by the definition of s' and $o_{\mathcal{R}}$,

$$\Pr(o_{\mathcal{R}}|s', a) = \Pr(\cup_{i=1}^N o_{\mathcal{R}_i}|s'_1, \dots, s'_N, \mathcal{M}) \quad (1)$$

We make a simplifying assumption that $o_{\mathcal{R}_i}$ is conditionally independent of all other $o_{\mathcal{R}_j}$ and s'_j ($j \neq i$) given s'_i and map \mathcal{M} . We make this assumption because the human observer is capable of producing a language $o_{\mathcal{R}_i}$ to describe target i given just the target location s_i and the map \mathcal{M} . This means

$$\Pr(\cup_{i=1}^N o_{\mathcal{R}_i}|s'_1, \dots, s'_N, \mathcal{M}) = \frac{1}{Z} \prod_{i=1}^N \Pr(o_{\mathcal{R}_i}|s'_i, \mathcal{M}) \quad (2)$$

where Z is the normalizing constant. Using the definition of $o_{\mathcal{R}_i}$, we take the following steps regarding $\Pr(o_{\mathcal{R}_i}|s'_i, \mathcal{M})$,

$$\Pr(o_{\mathcal{R}_i}|s'_i, \mathcal{M}) = \Pr(f_i, r_1, \gamma_1, \dots, r_L, \gamma_L|s'_i, \mathcal{M}) \quad (3)$$

$$= \Pr(r_1, \dots, r_L|\gamma_1, \dots, \gamma_L, f_i, s'_i, \mathcal{M}) \quad (4)$$

$$\times \Pr(\gamma_1, \dots, \gamma_L, f_i|s'_i, \mathcal{M}) \quad (4)$$

$$= \prod_{j=1}^L \Pr(r_j|\gamma_j, f_i, s'_i, \mathcal{M}) \quad (5)$$

The first term in (4) is factored by individual spatial relations, because each r_j is a predicate that, by definition, involves only the figure f_i and the ground γ_j , therefore it is conditionally independent of all other relations and grounds given f_i , its location s'_i , and the landmark γ_j and its features contained in \mathcal{M} . The second term in (4) is set to 1 because the robot has no prior knowledge regarding the human observer's language use¹, making $\Pr(\gamma_1, \dots, \gamma_L, f_i|s'_i, \mathcal{M})$ uniform.

For predicates like *behind*, its truth value depends on the relative FoR imposed by the human observer who knows the target location. Denote the FoR vector corresponding to r_j as a random variable Ψ_j that distributes according to the indicator function $\Pr(\Psi_j = \psi_j) = \mathbb{1}(\psi_j = \psi_j^*)$, where ψ_j^* is the one imposed by the human. Then regarding $\Pr(r_j|\gamma_j, f_i, s'_i, \mathcal{M})$, we can sum out Ψ_j :

$$\Pr(r_j|\gamma_j, f_i, s'_i, \mathcal{M}) = \frac{\sum_{\psi_j} \Pr(r_j, \gamma_j, f_i, s'_i, \mathcal{M}|\psi_j) \Pr(\psi_j)}{\Pr(\gamma_j, f_i, s'_i, \mathcal{M})} \quad (6)$$

$$= \frac{\Pr(r_j, \gamma_j, f_i, s'_i, \mathcal{M}|\psi_j^*)}{\Pr(\gamma_j, f_i, s'_i, \mathcal{M})} \quad (7)$$

$$= \Pr(r_j|\gamma_j, \psi_j^*, f_i, s'_i, \mathcal{M}) \quad (8)$$

(7) becomes (8) by law of total probability and then canceling the numerator and denominator terms, using the fact that s'_i, \mathcal{M} is independent of ψ_j^* , and that no prior knowledge

¹In general, the human observer may produce spatial language that mentions arbitrary landmarks and figures whether they make sense or not.

of ground γ_j and figure f_i used in the spatial language is given, similar to the justification from (4) to (5).

The observer's relative FoR ψ_j^* , by definition, depends on properties of both the ground, the figure and its true location, and the observer's subjective experience. The latter two are unknown to the robot. Therefore, we consider two subproblems: the approximation of ψ_j^* by a predicted value $\hat{\psi}_j$ and the modeling of $\Pr(r_j|\gamma_j, \hat{\psi}_j, f_i, s'_i, \mathcal{M})$. We describe our FoR prediction approach in the next section. We model $\Pr(r_j|\gamma_j, \hat{\psi}_j, f_i, s'_i, \mathcal{M})$ as a gaussian following prior work as well as evidence from animal behavior [13, 14]:

$$\Pr(r_j|\gamma_j, \hat{\psi}_j, f_i, s'_i, \mathcal{M}) = |u(s'_i, \gamma_j, \mathcal{M}) \cdot v(f_i, r_j, \gamma_j, \hat{\psi}_j)| \times \exp(-dist(s'_i, \gamma_j, \mathcal{M})^2/2\sigma^2) \quad (9)$$

where σ controls the steepness of the distribution based on landmark size, and $dist(s'_i, \gamma_j, \mathcal{M})$ is the distance between s'_i to the closest position within the ground γ_j in map \mathcal{M} , and $u(s'_i, \gamma_j, \mathcal{M}) \cdot v(f_i, r_j, \gamma_j, \hat{\psi}_j)$ is the dot product between $u(s'_i, \gamma_j, \mathcal{M})$, the unit vector from s'_i to the closest position within the ground γ_j in map \mathcal{M} , and $v(f_i, r_j, \gamma_j, \hat{\psi}_j)$, a unit vector in the direction that satisfies the semantics of the proposition (f_i, r_j, γ_j) by rotating $\hat{\psi}_j$. The precise definition of $\hat{\psi}_j$ is given in the section below. The dot product is dropped for predicates that do not require FoRs (e.g. *near*). We refer to Landau and Jackendoff [12] for a list of prepositions meaningful in 2D that require FoRs: *above, below, down, top, under, north, east, south, west, northwest, northeast, southwest, southeast, front, behind, left, right*.

C. Learning to Predict Latent Frame of Reference

Here we describe our approach to predict ψ_j^* corresponding to a given (f_i, r_j, γ_j) tuple, which is critical for correct resolution of spatial relations. Taking inspiration from the ice cream truck example where the tourist can infer a potential FoR by looking at the 2D map of the park, we train a model that predicts the human observer's imposed FoR based on the environment context embedded in the map.

We define an FoR in a 2D map as a single vector $\psi_j = (x, y, \theta)$ located at (x, y) at an angle θ with respect to the $+x$ axis of the map. We use the center-of-mass of the ground as the origin (x, y) . We make this approximation since our data collection shows that when looking at a 2D map, human observers tend to consider the landmark as a whole without decomposing it into parts. Therefore, the FoR prediction problem becomes a regression problem of predicting the angle θ given a representation of the environment context.

We design a convolutional neural network, which takes as input a grayscale image representation of the environment context where the ground in the spatial relation is highlighted. Surrounding landmarks are also highlighted with different brightness for streets and buildings (Figure 2). The image is shifted to be egocentric with respect to the referenced landmark, and cropped into a 28×28 pixel image. The intuition is to have the model focus on immediate surroundings, as landmarks that are far away tend not to

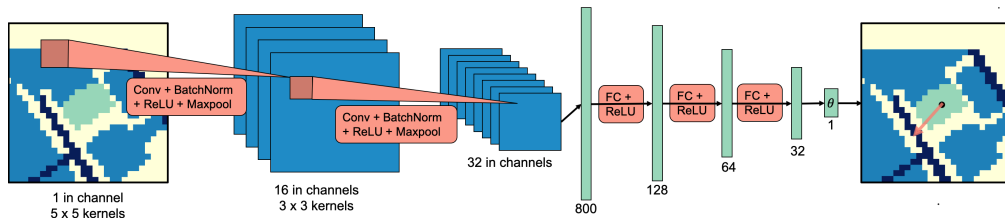


Fig. 2: **Frame of Reference Prediction Model Design.** In this example taken from our dataset, the model is predicting the frame of reference for the preposition *front*. The grayscale image is rendered with color ranging from blue (black), green (gray) to yellow (white). Green highlights the referenced landmark, dark blue the streets, blue the surrounding buildings, and yellow the background.

contribute to inferring the referenced landmark’s properties. The model consists of two standard convolution modules followed by three fully connected layers. These convolution modules extract an 800-dimension feature vector, feeding into the fully connected layers, which eventually output a single value for the FoR angle. We name this model **EGO-CTX** for egocentric shift of the contextual representation.

Regarding the loss function, a direct comparison with the labeled FoR angle is not desirable. For example, suppose the labeled angle is 0 (in radians). Then, a predicted angle of 0.5 is qualitatively the same as another predicted angle of -0.5 or $2\pi - 0.5$. For this reason, we apply the following treatment to the difference between predicted angle θ and the labeled angle θ^* . Here, both θ and θ^* have been reduced to be between 0 to 2π :

$$\ell(\theta, \theta^*) = \begin{cases} 2\pi - |\theta - \theta^*|, & \text{if } |\theta - \theta^*| > \pi, \\ |\theta - \theta^*|, & \text{otherwise} \end{cases} \quad (10)$$

This ensures that the angular deviation used to compute the loss ranges between 0 to π . The learning objective is to reduce such deviation to zero. To this end, we minimize the mean-squared error loss $L(\theta, \theta^*) = \frac{1}{N} \sum_{i=1}^N (\ell(\theta_i, \theta_i^*))^2$, where θ, θ^* are predicted and annotated angles with size N . This objective gives greater penalty to angular deviations farther away from zero.

In our experiments, we combine the data by antonyms and train two models for each baseline: a **front** model used to predict FoRs for *front* and *behind*, and a **left** model used for *left* and *right*². The training data for **front** is augmented by random rotations, whereas no data augmentation is performed for **left**. We use the Adam optimizer [15] to update the network weights with a fixed learning rate of 1×10^{-5} . Early stopping based on validation set loss is used with a patience of 20 epochs [16].

D. Spatial Information Extraction from Natural Language

We designed a pipeline to extract spatial relation triplets from the natural language using the spaCy library [17] for noun phrase (NP) identification and dependency parsing, as it achieves good performance on these tasks. Extracted NPs are matched against synonyms of target and landmark symbols using cosine similarity. All paths from targets to landmarks in

²We do not train a single model for all four prepositions since *left* and *right* often also suggest an *absolute* FoR used by the language provider when looking at 2D maps, while *front* and *behind* typically suggest a *relative* FoR.

the dependency parse tree are extracted to form the (f, r, γ) tuples used as spatial language observations (Section IV-B)

Our spatial language understanding models assume as input language that has been parsed into (f, r, γ) tuples, but is not dependent on this exact pipeline for doing so. Future work could explore alternative methods for parsing and entity linking, including approaches optimized for the task of spatial language resolution. In our end-to-end experiments, we report the task performance both when using this parsing pipeline and when using manually annotated (f, r, γ) tuples to indicate the influence of parsing on search performance.

V. DATA COLLECTION

We use maps from OpenStreetMap (OSM), a free and open-source database of the world map with voluntary landmark contributions [18]. We scrape landmarks in 40,000m² grid-regions with a resolution of 5m by 5m grid cells in five different cities leading to a dimension of 41×41 per grid map³: Austin, TX; Cleveland, OH; Denver, CO; Honolulu, HI, and Washington, DC. Geographic coordinates of OSM landmarks are translated into grid map coordinates.

To collect a variety of spatial language descriptions from each city, we randomly generate 30 environment configurations for each city, each with two target objects. We prompt Amazon Mechanical Turk (AMT) workers to describe the location of the target objects and specify that the robot knows the map but does not know target locations. Each configuration is used to obtain language descriptions from up to eleven different workers. The descriptions are parsed using our pipeline described in Section IV-D. Examples are shown in Figure 3. Screenshots of the survey and statistics of the dataset are provided in the supplementary video.

The authors annotated FoRs for *front*, *behind*, *left* and *right* through a custom annotation tool which displays the AMT worker’s language alongside the map without targets. We infer the FoR used by the AMT worker, similar to what the robot is tasked to do. This set of annotations are used as data to train and evaluate our FoR prediction model. Prepositions such as *north*, *northeast* have absolute FoRs with known direction. Others are either difficult to annotate (e.g. *across*) or have too little samples (e.g. *above*, *below*).

³Because of the curvature of the earth, the grid cells and overall region is not perfectly square, which is why the grid is not perfectly 40x40

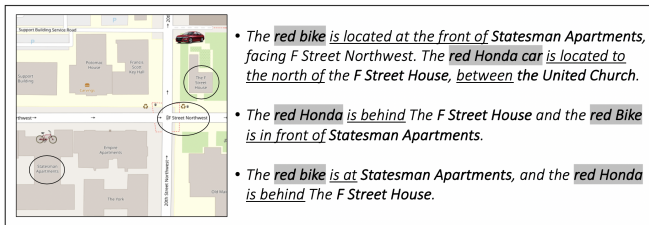


Fig. 3: Map screenshot shown to AMT workers paired with collected spatial language descriptions.

VI. EXPERIMENTS

A. Frame of Reference Prediction

We test the generalizability of our FoR prediction model (**EGO-CTX**) by cross-validation. The model is trained on maps from four cities and tested on the remaining held-out city for all possible splits. We evaluate the model by the angular deviation between predicted and annotated FoR angles, in comparison with three baselines and human performance: The first is a variation (**CTX**) that uses a synthetic image with the same kind of contextual representation yet without egocentric shift. The second is another variation (**EGO**) that performs egocentric shift and also crops a 28×28 window, but only highlights the referenced landmark at the center without contextual information. The random baseline (**Random**) predicts the angle at random uniformly between $[0, 2\pi]$. The **Human** performance is obtained by first computing the differences between pairs of annotated FoR angles for the same landmarks (Equation 10), then averaging over all such differences for landmarks per city. Each pair of FoRs may be annotated by the same or different annotators. Taking the average gives a sense of the disagreement among the annotators' interpretation of spatial relations.

The results are shown in Figure 4. Each boxplot summarizes the means of baseline performance in the five cross-validation splits. The results demonstrate that **EGO-CTX** shows generalizable behavior close to the human annotators, especially for **front**. We observe that our model is able to predict *front* FoRs roughly perpendicular to streets against other buildings, while the baselines often fail to do so (Figure 5). The competitive performance of the neural network baselines in **left** indicates that for *left* and *right*, the FoR annotations are often absolute, i.e. independent of the context.

B. End-to-End Evaluation

We randomly select 20 spatial descriptions per city. We task the robot to search for each target object mentioned in every description separately, resulting in a total of 40 search trials per city, 200 in total. Cross-validation is employed such that for each city, the robot uses the FoR prediction model trained on the other four cities. For each step, the robot can either move or mark an object as detected. The robot can move by rotating clockwise or counterclockwise for 45 degrees, or move forward by 3 grid cells (15m). The robot receives observation through an on-board fan-shaped sensor after every move. The sensor has a field of view with an angle of 45 degrees and a varying depth of 3, 4, 5 (15m,

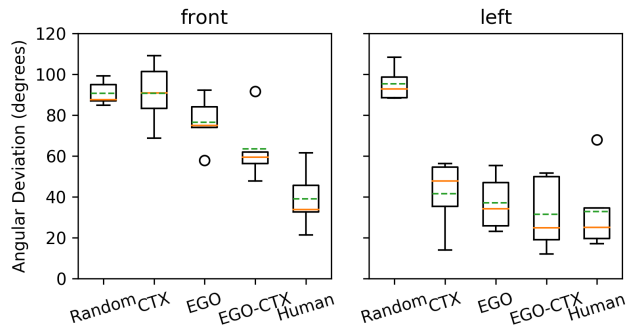


Fig. 4: FoR prediction results. The solid orange line shows the median, and the dotted green line shows the mean. The circles are outliers. Lower is better.

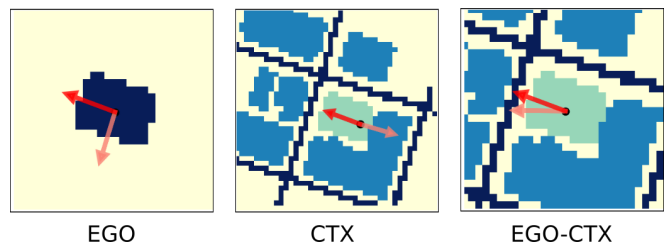


Fig. 5: Visualization of FoR predictions for *front*. Darker arrows indicate labeled FoR, while brighter arrows are predicted FoR.

20m, 25m). As the field of view becomes smaller, the search task is expected to be more difficult. The robot receives -10 step cost for moving and $+1000$ for correctly detecting the target, and -1000 if the detection is incorrect. The rest of the domain setup follows [5].

We compare the search performance using our spatial language understanding model (**slu**) against three models. The first is an upper bound (**informed**) in which the agent knows the ground-truth location of the target objects with some noise. The second (**keyword**) uses a keyword-based model [5] that assigns a uniform probability over referenced landmarks in a spatial language but does not incorporate information from spatial prepositions. The third baseline (**uniform**) uses a uniform prior. We also report the performance of our system and keyword using the same languages but with annotated spatial relations (**slu, annotated** and **keyword, annotated**). Our parsing pipeline attains a precision/recall of 100%/88.9% for recognizing referenced landmarks and 88.9%/76.2% for recognizing spatial relation propositions (i.e. (f, r, γ) tuples) for selected languages.

For all baselines, we use an online POMDP solver, POMCP [19] but with a histogram belief representation to avoid particle depletion. The number of simulations per planning step is 1000 for all baselines. The discount factor is set to 0.95. The robot is allowed to search for 200 steps per search task, since search beyond this point will earn very little discounted reward and is not efficient.

We evaluate the *effectiveness* and *efficiency* of the search by the amount of search tasks the robot completed (i.e. successfully found the target) under a given limit of search steps (ranging from 1 to 200). Results are shown in Figure 7. Our system performs better compared to the **keyword** base-

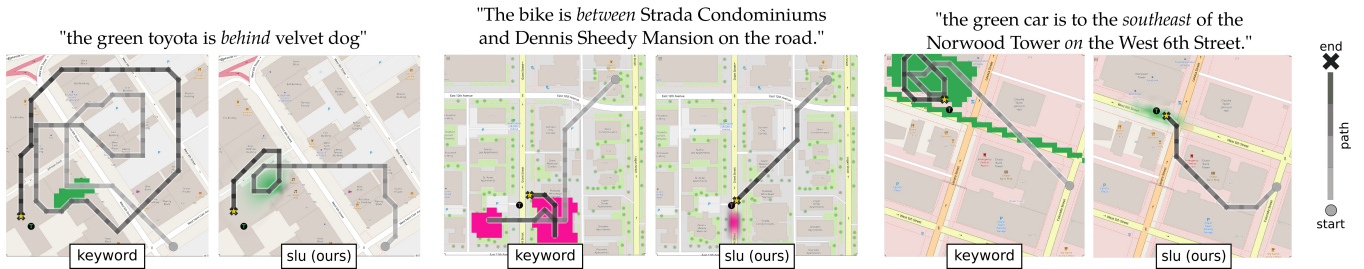


Fig. 6: Example object search trials in end-to-end evaluation. The search path is overlaid on top of the initial belief formed by interpreting the given spatial language. The robot eventually finds the target. However, our system leads to more efficient search policies.

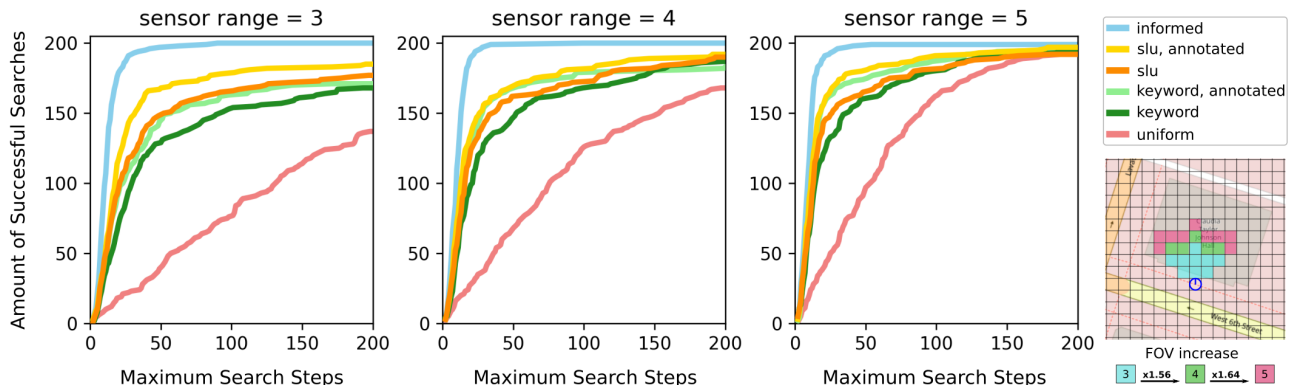


Fig. 7: Number of completed search tasks as the maximum search step increases. Steeper slope indicates greater efficiency and success rate of search. Our system **slu** performs better compared to the **keyword** baseline with increasing margin as the sensor range decreases.

predicate	#trials	keyword	slu	keyword, annotated	slu, annotated
on	177	292.17 (51.35)	372.45 (54.68)	314.98 (45.11)	372.28 (43.24)
at	174	341.26 (50.95)	312.76 (52.67)	302.12 (47.21)	328.32 (47.03)
near	105	154.50 (60.79)	206.40 (63.07)	263.33 (75.65)	361.21 (66.21)
between	75	-41.27 (52.25)	248.87 (84.08)	221.57 (79.17)	254.38 (86.79)
in	66	206.64 (79.69)	250.70 (78.96)	443.81 (70.26)	456.82 (65.74)
beside	24	276.82 (147.70)	390.48 (100.31)	365.11 (115.04)	545.81 (70.10)
next	21	122.88 (150.12)	291.61 (118.07)	407.40 (123.83)	395.07 (113.40)
along	18	255.46 (208.93)	385.34 (166.27)	358.21 (155.54)	459.17 (114.34)
north	27	68.58 (132.67)	138.82 (142.22)	371.42 (136.69)	355.70 (146.34)
southeast	21	169.52 (155.36)	386.10 (89.69)	310.52 (154.15)	576.28 (73.78)
southwest	21	74.19 (167.30)	27.35 (175.15)	-20.39 (123.52)	26.62 (140.17)
east	18	238.88 (185.02)	423.14 (121.50)	249.48 (185.15)	449.82 (143.53)
northwest	18	533.63 (163.69)	406.41 (242.40)	378.86 (149.98)	190.25 (178.59)
south	18	474.61 (218.73)	536.51 (177.22)	236.59 (182.40)	498.47 (143.91)
west	12	-74.11 (168.83)	437.23 (100.03)	80.88 (171.88)	403.38 (189.28)
front	75	299.39 (77.26)	229.15 (93.85)	324.56 (75.22)	208.91 (81.76)
behind	24	-54.43 (106.10)	85.89 (129.08)	191.01 (170.09)	143.99 (162.78)
right	12	203.15 (198.98)	75.55 (212.87)	348.70 (263.77)	228.27 (237.47)
left	9	11.23 (195.65)	90.18 (224.12)	351.08 (133.68)	275.28 (187.04)
front (good)	45	373.06 (101.39)	432.56 (105.91)	370.55 (95.47)	444.14 (69.77)
behind (good)	18	-62.43 (137.89)	87.09 (125.82)	174.74 (223.81)	263.25 (186.60)
front (bad)	30	188.89 (114.41)	-75.97 (102.62)	255.58 (124.60)	-143.94 (59.95)
behind (bad)	6	-30.41 (175.88)	82.28 (483.35)	239.83 (243.65)	-213.79 (7.63)

TABLE I: Mean (95% CI) of discounted cumulative reward per preposition, averaging over trials from all sensor ranges.

line with increasing margin as the sensor range decreases. The gain in the discounted reward is statistically significant over all sensor ranges comparing **slu** with **keyword**, and for sensor range 3 comparing the annotated versions. We observe improvement when the system is given annotated spatial relations. This suggests the important role of language parsing for spatial language understanding. Example search trials comparing **slu** and **keyword** are shown in Figure 6.

We analyze the performance with respect to different spatial predicates, Results over all sensor ranges are given in Table I. Our system outperforms **keyword** for most of the prepositions. For prepositions *front*, *behind*, *left*, and *right*, our investigation shows the performance of **slu** polarizes where trials with “good” FoR (i.e. ones in the correct

direction towards the true target location) leads to a much greater performance than the counterpart (“bad” FoR). Yet, **keyword** is not subject to such polarization and the target often appears close to the landmark for these prepositions. One limitation of our FoR prediction method is that it is not probabilistic. Future work can investigate planners that can consider multiple FoR candidates.

Finally, we analyze the relationship between the performance and varying complexity of the language description, indicated by the number of spatial relations used to describe the target location. Results show **slu** outperforms **keyword** for all language complexity settings. We observe an increase in the performance of **slu** when the number of spatial relations goes from 1 to 2 (from 284.67 ± 38.62 to 320.92 ± 43.37), yet a decrease in performance for more complex descriptions (202.86 ± 127.59 at 3 and 140.70 ± 389.61 at 4). This demonstrates a limitation of our system where interpretation of many conjunctive spatial relations leads to a small concentration in the belief that deviates from the actual target location. Future work can explore ways of using parts of the spatial information at a time, instead of all at once.

VII. CONCLUSIONS

This paper first presents formalism for integrating spatial language into the POMDP belief state as an observation, then a convolutional neural network for FoR prediction shown to generalize well to new cities. End-to-end experimentation shows that our system significantly improves object search efficiency and effectiveness in cityscale domains through understanding spatial language.

REFERENCES

- [1] S. Tellex, T. Kollar, S. Dickerson, M. R. Walter, A. G. Banerjee, S. Teller, and N. Roy, "Understanding natural language commands for robotic navigation and mobile manipulation," in *National Conference on Artificial Intelligence*. Association for the Advancement of Artificial Intelligence, 2011.
- [2] J. Fasola and M. J. Matarić, "Using spatial semantic and pragmatic fields to interpret natural language pick-and-place instructions for a mobile service robot," in *International Conference on Social Robotics*. Springer, 2013, pp. 501–510.
- [3] S. Hemachandra, F. Duvall, T. M. Howard, N. Roy, A. Stentz, and M. R. Walter, "Learning models for following natural language directions in unknown environments," in *2015 IEEE International Conference on Robotics and Automation (ICRA)*. IEEE, 2015, pp. 5608–5615.
- [4] S. Patki, E. Fahnstock, T. M. Howard, and M. R. Walter, "Language-guided semantic mapping and mobile manipulation in partially observable environments," in *Conference on Robot Learning*, 2020, pp. 1201–1210.
- [5] A. Wandzel, Y. Oh, M. Fishman, N. Kumar, W. Lawson L.S., and S. Tellex, "Multi-object search using object-oriented pomdps," in *2019 International Conference on Robotics and Automation (ICRA)*, May 2019, pp. 7194–7200.
- [6] L. P. Kaelbling, M. L. Littman, and A. R. Cassandra, "Planning and acting in partially observable stochastic domains," *Artificial Intelligence*, vol. 101, no. 1, pp. 99–134, 1998.
- [7] T. Kollar, S. Tellex, D. Roy, and N. Roy, "Toward understanding natural language directions," in *2010 5th ACM/IEEE International Conference on Human-Robot Interaction (HRI)*. IEEE, 2010, pp. 259–266.
- [8] A. Boularias, F. Duvall, J. Oh, and A. Stentz, "Learning qualitative spatial relations for robotic navigation," in *Proceedings of the Twenty-Fifth International Joint Conference on Artificial Intelligence*, ser. IJCAI'16. AAAI Press, 2016, p. 4130–4134.
- [9] J. Thomason, M. Murray, M. Cakmak, and L. Zettlemoyer, "Vision-and-dialog navigation," in *Conference on Robot Learning (CoRL)*, 2019.
- [10] A. Majid, M. Bowerman, S. Kita, D. B. Haun, and S. C. Levinson, "Can language restructure cognition? the case for space," *Trends in cognitive sciences*, vol. 8, no. 3, pp. 108–114, 2004.
- [11] A. Shusterman and P. Li, "Frames of reference in spatial language acquisition," *Cognitive psychology*, vol. 88, pp. 115–161, 2016.
- [12] B. Landau and R. Jackendoff, "'what' and 'where' in spatial language and spatial cognition," *Behavioral and Brain Sciences*, vol. 16, pp. 217–265, 06 1993.
- [13] J. Fasola and M. J. Matarić, "Using semantic fields to model dynamic spatial relations in a robot architecture for natural language instruction of service robots," in *2013 IEEE/RSJ International Conference on Intelligent Robots and Systems*. IEEE, 2013, pp. 143–150.
- [14] J. O'Keefe and N. Burgess, "Geometric determinants of the place fields of hippocampal neurons," *Nature*, vol. 381, no. 6581, pp. 425–428, 1996.
- [15] D. P. Kingma and J. Ba, "Adam: A method for stochastic optimization," in *International Conference on Learning Representations (ICLR)*, 2015.
- [16] L. Prechelt, "Early stopping-but when?" in *Neural Networks: Tricks of the trade*. Springer, 1998, pp. 55–69.
- [17] M. Honnibal and I. Montani, "spaCy 2: Natural language understanding with Bloom embeddings, convolutional neural networks and incremental parsing," 2017, to appear.
- [18] OpenStreetMap contributors, "Planet dump retrieved from <https://planet.osm.org>," 2017.
- [19] D. Silver and J. Veness, "Monte-carlo planning in large pomdps," in *Advances in neural information processing systems*, 2010, pp. 2164–2172.